CHAPTER II
THEORETICAL BACKGROUND AND LITERATURE REVIEW

2.1 Polycarbonate (PC)

Polycarbonate was discovered in 1953 by r. H. Schnell at Bayer AG, Germany, and by D. W. Fox at General Electric Company, USA working independently, this name originates from consisting of carbonate group in the structure, which is one of the most widely used engineering plastics because of its unique properties. It is most commonly synthesized by the reaction of bisphenol A and phosgene ($COCl_2$) in an interfacial polymerization process as shown in Figure 2.1.
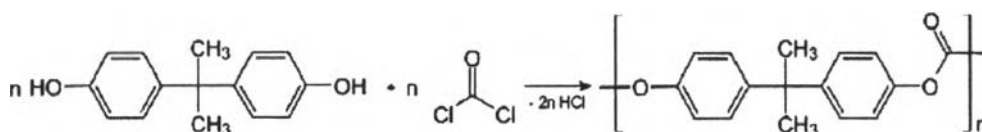

Figure 2.1 The overall reaction of polycarbonate.

Aromatic polycarbonate that derived from bisphenol A becomes more interesting because it has many useful properties for example, it has rigid molecule structure in the backbone chain and it is amorphous polymer, leading to high optical transparency. Furthermore, it is well known in exceptional impact resistance and also offers excellent moldability and extrudability. Other properties such as modulus and tensile strength are comparable to other amorphous polymers (T_g). While most amorphous polymers are stiff and brittle below their T_g values, polycarbonates still retain their ductility and impact resistance below their T_g values. Polycarbonate was initially used for electrical and electronic applications and subsequent glazing for greenhouses and buildings. A major application of polycarbonate is the production of data storage like compact discs. Nowadays, polycarbonate is outstanding combination of beneficial characteristics made it as the candidates for many other applications such as automotive, aircraft, and security components.

2.2 Poly(methyl methacrylate) (PMMA)

The polymerization of Poly(methyl methacrylate) from methyl methacrylate was discovered in 1877 by the German chemists Fittig and Paul and was developed continuously. In 1933, the Rohm and Haas Company first brought PMMA to market under the trademark Plexiglas. It is often generally called acrylic glass even though it is chemically unrelated to glass. PMMA is regularly produced by emulsion polymerization, solution polymerization and bulk polymerization. Radical initiation is generally used which PMMA produced by polymerization, all commercial PMMA, is atactic and completely amorphous. It is a glass-clear, transparent thermoplastic, which is limited by its relatively poor dimensional stability low impact strength and low temperature stability. However, it is well known in surface hardness, UV resistance and generally good weather ability and chemical resistance. That is why PMMA is widely used in many applications such as window glazings, aircraft windows, and automotive lenses or lightcovers.

2.3 Polymer Alloys Definition

Polymer alloy is an immiscible or compatibilized polymer blend, which has a modified interface and morphology or a blend that is stabilized by covalent bond or ionic bond formation between phases or by attractive intermolecular interaction. It can improve the specific properties such as impact strength and scratch resistance. Polymer alloy is not only called blend or polyblend but is also usually designed to maintain the best characteristics of each material, which can be identified, by these characteristics; the mixture is totally mechanical and also has to have a single melt-transition temperature. In addition, at least one property or characteristic of the base polymer is improved synergistically by the addition of the other polymers. If synergistic improvement is not achieved, at least the best properties of all constituents are still retained. The most improvements of properties that have been found are impact strength, heat-deflection temperature, flame retardance, chemical and weather resistance, and processibility.

2.4 Polycarbonate/ Poly(methyl methacrylate) alloys system

PC/PMMA blends are extensively used as high performance plastics, which provide the high transparency and scratch resistance of PMMA combine with the excellent properties of PC such as outstanding ductility and high T_g. Because of their superior properties, these materials participate in many potential applications as gas separation membrane, substrate of the optical data storage discs and pearl and packaging material.

In 2009, Manasvi *et al.* studied about PMMA/PC blends and focused on morphology, miscibility and mechanical properties. The films of PMMA/PC blends were prepared by solution casting technique, which had compositions of 100/0, 75/25, 50/50, 25/75 and 0/100 by weight at 50°C temperature and used tetrahydrofuran (THF) as solvent. For the miscibility of the blends, the glass transition of the systems was observed by using DMA and DSC. A single glass transition temperature in all the blends was reported in DMA results and from Figure 2.2 DSC thermogram of 75PMMA/25PC, 50PMMA/50PC and 25PMMA/75PC blends, also showed the single glass transition temperature of PMMA/PC blends, which suggested that these blends were good compatible blends, which the values of the glass transition temperature of PMMA/PC blends were given in Table 2.1.

Table 2.1 Glass transition temperature of PMMA, PC and their blends

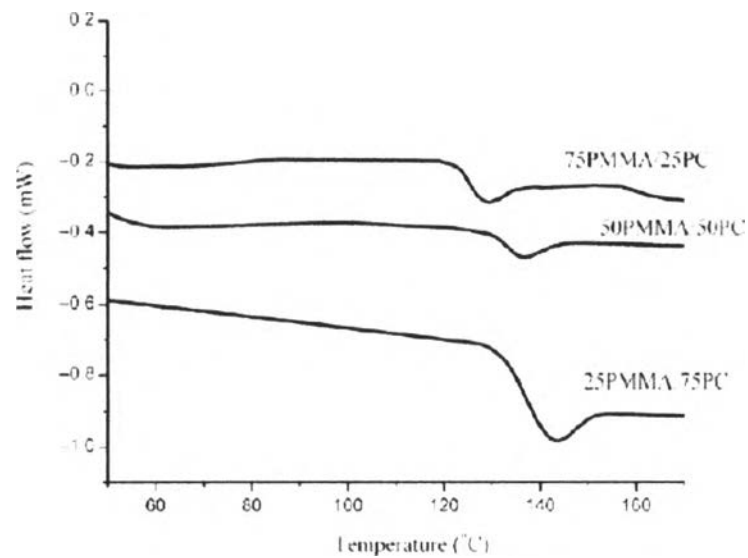| Sample	Glass transition temperature (T_b)
100PMMA	83.8
75PMMA 25PC	129.55
50PMMA 50PC	133.21
25PMMA 75PC	149.40
100PC	150.5

Figure 2.2 DSC thermogram of 75PMMA/25PC, 50PMMA/50PC and 25PMMA/75PC blends.

In morphological investigation, SEM micrographs showed very fine phase morphology, the unclear observation in boundary between PMMA and PC, in the fractured surface of PMMA/PC blends (Figure 2.3). The result meant that the PC was compatible with PMMA.
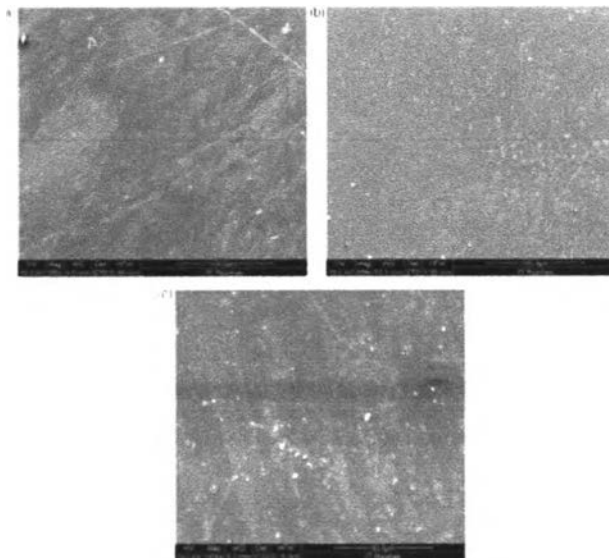
Figure 2.3 (a) SEM micrographs of 75PMMA/25 PC. (b) SEM micrographs of 50PMMA/50 PC. (c) SEM micrographs of 25PMMA/75 PC.

The mechanical properties showed that the modulus and strength of PMMA/PC blends was influenced by composition and followed a synergic behavior (Figure 2.4, Table 2.2). The higher value of mechanical properties for 75PMMA/ 25PC indicated the better quality of this blend. It could be concluded that increasing of PC content in PMMA matrix reduced the mobility of main chain movements and enhanced the toughness of PMMA/PC blends.
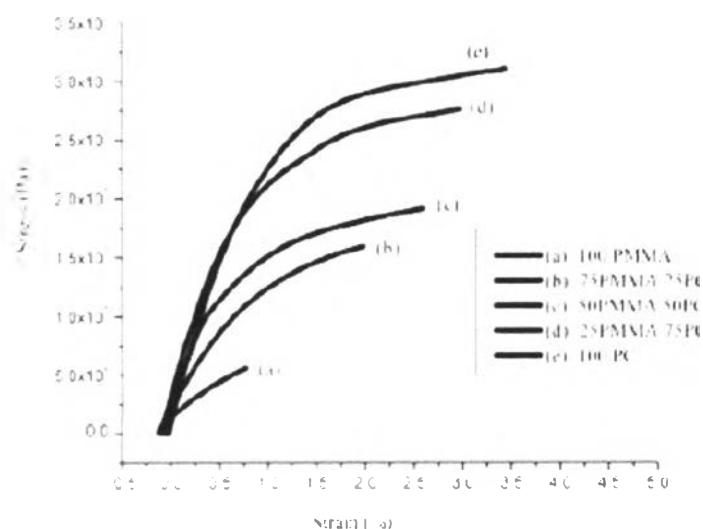
Figure 2.4 Tensile stress–strain curve for PMMA/PC blends.

Table 2.2 Mechanical properties of PMMA, PC and their blends

Sample	Young's modulus (GPa)	Ultimate tensile strength (MPa)	Elongation at break (%) at room temperature	Fracture energy (10^{-3} J)
100PMMA	0.70	5.69	0.76	0.31
75PMMA 25PC	1.85	18	1.99	0.62
50PMMA 50PC	2.37	21.3	2.61	1.10
25PMMA 75PC	2.53	23	2.97	1.74
100PC	1.18	30.8	3.41	1.98

2.5 Immiscibility problems in PC/PMMA alloys

Mixing of two polymers usually result in a completely miscible, partially miscible or immiscible system. The properties of polymer blends are determined mainly by the miscibility of the components and structure, which strongly depend on polymer-polymer interaction. The miscibility is the same as thermodynamic solubility that two polymers are miscible in each other, which is determined by the free energy of mixing (ΔG_{mix}) which includes both entropic and enthalpic terms $(\Delta S_{mix}$ and $\Delta H_{mix})$.

$$\Delta G_{mix} = \Delta H_{mix} - T\Delta S_{mix}$$

$$= \Delta E_{mix} + P\Delta V_{mix} - T\Delta S_{mix}$$

If the free energy of mixing is negative, it means that the two polymers are miscible. While miscibility has a strict thermodynamic meaning, compatibility is defined in operational terms. A blend can be more or less compatible if it is closer or further from miscibility. So a completely compatible system is a miscible one. The compatibility of two polymers of a particular blend can be related to how good a particular property is.

In miscible blends, for which $\Delta H_{mix} < 0$, due to specific interactions, homogeneity is observed at least at the nanometer scale, if not at the molecular level which most polymer pairs form immiscible blend.

For PC/PMMA blend system, this system has been investigated extensively, serveral debates continue to abound the literature. PC/PMMA blend is generally prepared by melt extrusion or solution casting technique with or without compatibilizers. Although this blend is considered as an immiscible system, the work of Butzbach and Wendorff reported weak specific interactions between phenyl ring of PC and carbonyl group of PMMA phase. Kim *et al* also proposed that the compatibility in PC/PMMA blends would increase when the PMMA content increased, which meant the PMMA rich phase was more compatible than the PC rich phase. In order to improve a technological compatibility of immiscible polymer is to stabilize an appropriate morphology of the dispersed phase polymer in the matrix polymer by promotion of interphase adhesion or by lowering the interfacial tension.

2.6 Compatibilization process

Compatibilization is process of modification of the interfacial properties in immiscible polymer blend, resulting in reduction of the interfacial tension coefficient and stabilization of the desired morphology, thus leading to the creation of a polymer alloy.

There are three purposes for the compatibilization process:

    i.   To adjust the interfacial tension, thus generate the desired degree of dispersion.

    ii.   To make reliable that the morphology generated during the alloying stage will yield optimum structure during the forming stage.

iii. To enhance adhesion between the phases in the solid state, facilitating the stress transfer hence improving the properties of the blend.

The compatibilization processes can be divided into two categories:

2.6.1 Reactive Compatibilization

The reactive compatibilization is logically a sub-category of interchain copolymer formation reactions. Copolymer formation by reactive compatibilization is a heterogeneous reaction occurring across a melt phase boundary. This process often takes place by direct reaction between chemical functionalities on each of two polymers. It has some cases that a third reactive species is added into the blend to promote copolymer formation.

In 2010, Inpota *et al.* studied the effect of samarium(III)acetylacetonate (SMACA) catalyst on the mechanical properties and thermal properties of PC/PET alloys. The PC/PET blends with different weight ratio were prepared by mixing in twin screw extruder. SMACA was used as a transesterification catalyst to induce transesterification between PC and PET. From DSC results as shown in Table 2.3 they were found that the addition of SMACA into PC/PET systems showed single T_g at all compositions. In the case of PC80/PET20 with 0.025%Sm, it exhibited T_g value in between PC and PET and also closed to T_g of Fox's equation (Table 2.4). It can be noted that the miscibility of PC/PET alloys was improved by adding SMACA.

Table 2.3 DSC results of PC/PET alloys with SMACA

Formula	$T_{g,PET}$ (°C)	$T_{g,PC}$ (°C)	$T_{g,Alloys}$ (°C)	T_m (°C)	T_c (°C)	ΔH_m (J/g)	ΔH_c (J/g)	Crystallinity (%)
PC80	81.3	141.7	-	233.2	146.8	7.12	10.38	5.08
PC80 0.025Sm	-	-	119.5	231.5	127.4	1.97	5.96	1.41
PC80 0.050Sm	-	-	119.1	-	126.1	-	5.74	-
PC80 0.075Sm	-	-	120.1	-	127.1	-	3.98	-
PC50	81.6	Δ	-	238.6	148.7	22.55	10.07	16.10
PC50 0.025Sm	-	-	93.2	229.3	107.4	1.49	7.44	1.06
PC50 0.050Sm	-	-	101.1	-	107.6	-	7.44	-
PC50 0.075Sm	-	-	98.6	-	104.6	-	9.7	-
PC20	83.2	Δ	-	241.4	156.7	27.69	15.79	19.76
PC20 0.025Sm	-	-	86.1	226.9	90.1	19.21	1.96	13.71
PC20 0.050Sm	-	-	85.2	218.6	89.5	8.04	6.09	5.74
PC20 0.075Sm	-	-	84.9	219.9	90.0	0.61	5.56	0.44

ΔH of 100% crystalline PET is 140.1 J/g.

$^\Delta$ $T_{g,PC}$ was duplicated by cold crystallization temperature (T_{cc}).

Table 2.4 T_g of PC/PET alloys by calculation from Fox's equation.

Formula	$T_g(^\circ C)$ Fox's equation
PC80	126.6
PC50	106.4
PC20	91.7

Fox's equation: $1/T_g = W_{PET}/T_{g,PET} + W_{PC}/T_{g,PC}$

The transesterification reaction between PC and PET can be confirmed by using FT-IR as shown in Figure 2.5. In the case of PC/PET alloys in the presence of SMACA, arylate ester and alkyl-aryl carbonate were observed at 1735 and 1770 cm^{-1}, which resulted from the ester-ester exchange of transesterification reaction. Thus, it could be suggest that SMACA is one of the effective catalysts for blending PC and PET by generating PC/PET copolymer.
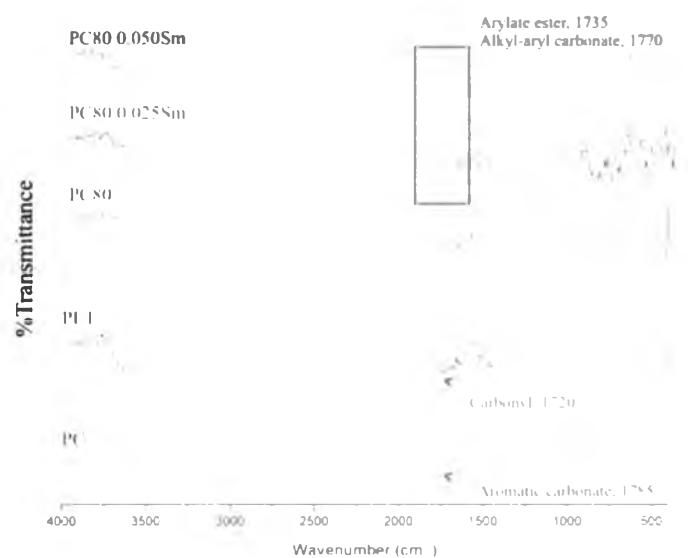
Figure 2.5 FT-IR spectra of PC, PET, PC80, PC80 0.025%Sm, and PC80 0.050%Sm.

Figure 2.6 revealed the impact strength of PC/PET alloys with SMACA. There was only one composition, PC80/PET20 with 0.025%SMACA, gave the impact strength

closed to neat PC, More than 0.025%SMACA of PC80, the impact strength dropped down which closed to its alloy without catalyst. So it indicated that the excess of catalyst reduced the impact strength because of a large number of PC/PET copolymers.
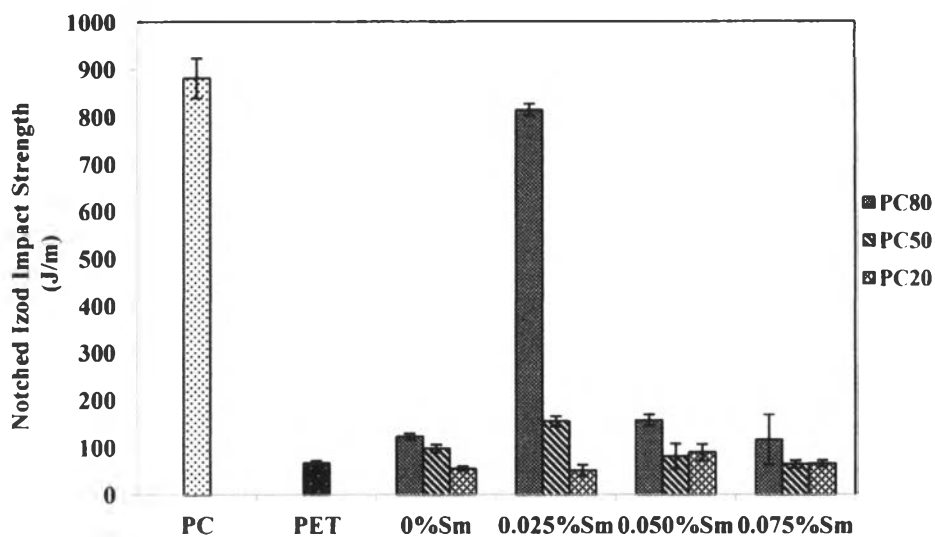

Figure 2.6 Notched izod impact strength of PC/PET alloys with SMACA.

It could be concluded that SMACA is the effective catalyst for reactive compatibilization of PC/PET alloys. After adding SMACA into the alloys, the single T_g was observed which indicated the miscibility was improved. In the case of impact properties, high impact strength was found at only PC80 with 0.025%SMACA composition. It seemed that the content of SMACA was not proper for the other alloys, resulting in lower impact properties.

In 2011, Singh *et al.* studied about reactive compatibilization of polycarbonate and poly(methyl methacrylate) in presence of a novel transesterification catalyst ($SnCl_2.2H_2O$). The PC/PMMA blends with different weight ratios were prepared by melt extrusion method. For DSC result from the second run (Figure 2.7) showed two distinguishable glass transition temperatures of PC/20PMMA without transesterification catalyst which both of the T_g values were shifted toward each other with respect to the pure polymers. It should be noted that some interaction between PC and PMMA in the melt extruded PC/20PMMA.

Besides, PC/20PMMA blends with transesterification catalysts (TBATPB and titanium butoxide) also showed two distinguishable glass transition temperatures similar to PC/20PMMA without transesterification catalyst, which suggested that the effect of these transesterification catalysts on compatibility of this PC/PMMA blend was trivial when used in 0.5% (wt/wt) ratio. On the other hand, PC/20PMMA blend was prepared by using $SnCl_2.2H_2O$ as transesterification catalyst in 0.5% (wt/wt) showed only single glass transition temperature, which decreased drastically with respect to T_g of PC. It pointed that the working of $SnCl_2.2H_2O$ was very efficiently in order to form the homogeneous of PC/PMMA blends.
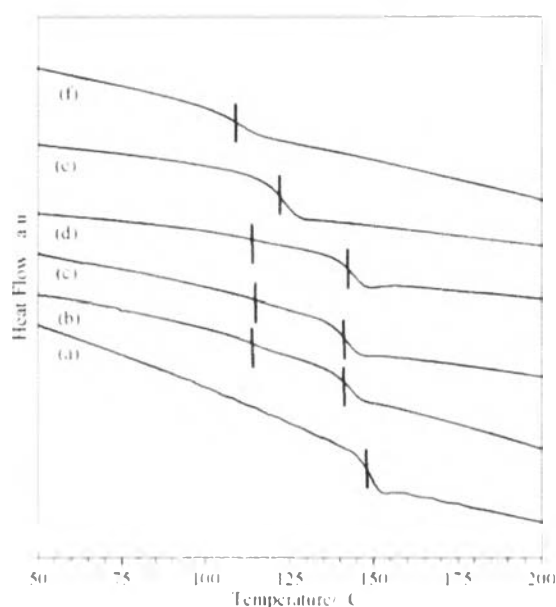
Figure 2.7 DSC thermograms (second run) of quenched PC/PMMA blends prepared by melt extrusion technique: **(a)** Pure PC, **(b)** PC/20PMMA blend, **(c)** PC/20PMMA + 0.5% tetrabutylammonium tetraphenylborate (TBATPB), **(d)** PC/20PMMA + 0.5% titanium butoxide, **(e)** PC/20PMMA + 0.5% $SnCl_2.2H_2O$ and **(f)** pure PMMA.

To realize the mechanism of possible interchange reaction between PC and PMMA phases in presence of $SnCl_2.2H_2O$, the researchers chose ^1H NMR spectra (Figure 2.8) to study on pure PC, pure PMMA and the homogeneous PC/PMMA blends with single T_g. Figure 2.8a showed the characteristic proton peaks of pure PC. The aromatic protons of PC were in two different environments which shown as 1 and 1' in Scheme 1. In pure PMMA (Figure 2.8b), there were three different proton environments, which corresponded to methyl ester, methyl and methylene shown as 3, 4, and 5 in Scheme 1. In presence of catalyst, the PC chain was informed to break at (-O-CO-O-) site. The two broken components were reported to link with methyl ester group in PMMA and still remain a part of PMMA chain as shown in Scheme 1. If a grafting of PC and PMMA occurs, the environment of methyl ester protons will change with respect to that in pure PMMA chain. This change of environment was demonstrated in Figure 2.8c, which it had not so many peaks were presented in the 1H NMR spectrum of this blend. Therefore, the grafting of PC and PMMA in presence of $SnCl_2.2H_2O$ occurred by the cleavage of the bonds in the neighborhood of (-O-CO-O-) of PC chain and its linkage with the methyl ester group of PMMA chain. It suggested that the grafted macromolecules acted as compatibilizers, which further increased the homogeneity of PC/PMMA blends.
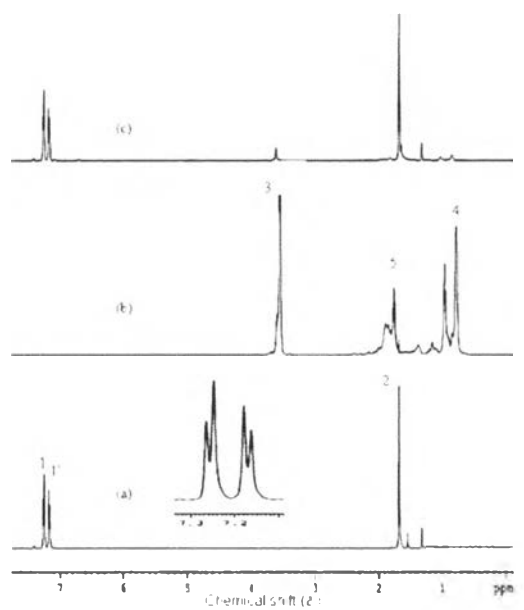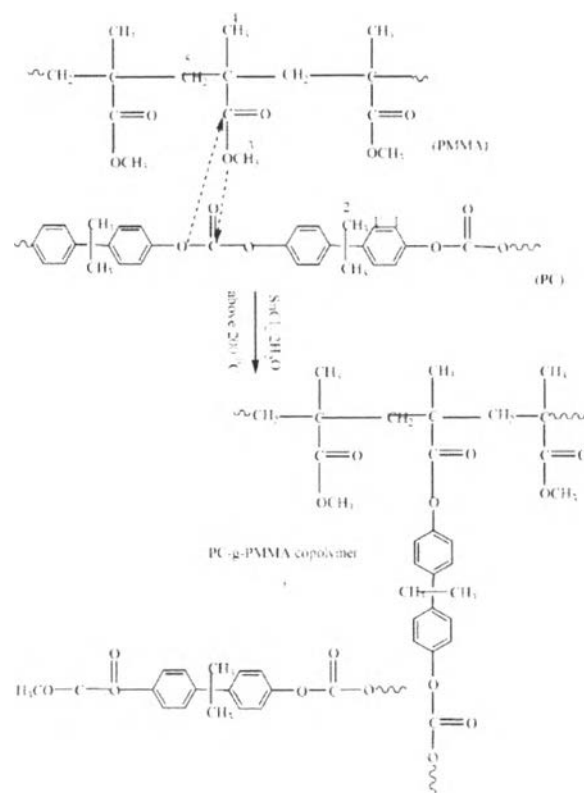
Figure 2.8 ^{1}H NMR spectrum of **(a)** PC, **(b)** PMMA and **(c)** PC/10PMMA + 0.3% SnCl$_2$.2H$_2$O transesterification catalyst. Inset of Figure 2.8a shows the zoomed NMR spectrum of PC in the range of 7.1 to 7.3 ppm.

Scheme 1. Mechanism of PC-g-PMMA Graft Copolymer Formation.

In order to confirm the mechanism of PC-g-PMMA graft copolymer formation, acetone was chosen as a solvent to leach PMMA out from the PC/PMMA blends because acetone acted as a good solvent for PMMA and non-solvent for PC. Then, these unleached and acetone-leached PC/PMMA blends were characterized by using FTIR technique (Figure 2.9). The FTIR spectra of the PC/20PMMA blends in Figure 2.9b showed two clear carbonyl stretching vibration peaks which corresponded to the carbonyl group of PC and PMMA, respectively. In contrast, the same sample after acetone leaching showed only the carbonyl peak of PC (Figure 2.9c). The FTIR spectra of the acetone-insoluble portion of PC/20PMMA + 0.3% $SnCl_2.2H_2O$ showed both carbonyl peaks of PC and PMMA as can be seen in Figure 16a. Moreover, the intensity of PMMA carbonyl peak in leached sample decreased significantly comparing with the unleached sample.
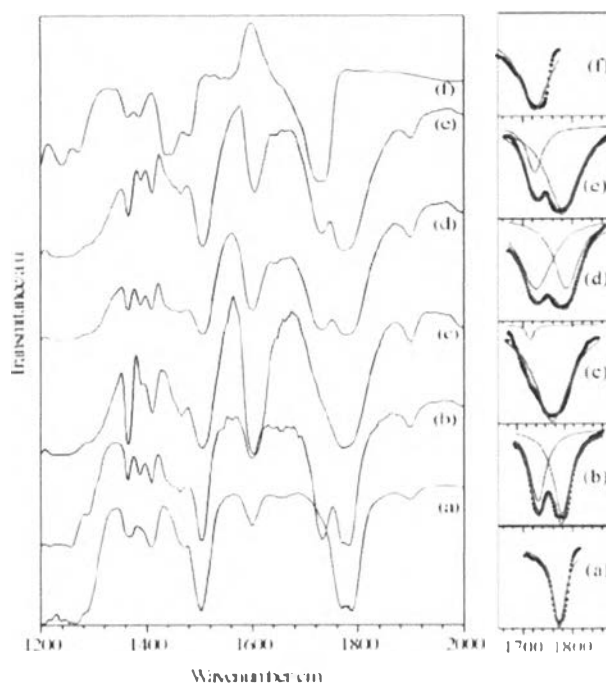
Figure 2.9 FTIR spectra of: **(a)** pure PC, **(b)** PC/20PMMA, **(c)** acetone insoluble portion of PC/20PMMA, **(d)** PC/20PMMA + 0.3% $SnCl_2.2H_2O$, **(e)** acetone insoluble portion of PC/20PMMA + 0.3% $SnCl_2.2H_2O$ and **(f)** pure PMMA prepared by melt extrusion method. In the right side, we have given the deconvoluted profile of the carbonyl peaks.

The thermal degradation of PC beads, extruded PC, extruded PC/20PMMA, extruded PC/20PMMA + 0.3% $SnCl_2.2H_2O$ and PMMA beads were studied by using TGA as shown in Figure 2.10. The TGA thermograms showed a decrease in the degradation temperature of extruded PC with respect to the PC beads. This might be due to the conversion of conformation take place during the extrusion process leading to the degradation of the material at a lower temperature. The PC/20PMMA blend without transesterification catalyst showed two steps thermal degradation, which corresponded to PC and PMMA, indicating insignificant interaction between the two phased. Whereas, the PC/20PMMA blend with 0.3% $SnCl_2.2H_2O$ showed a single step thermal degradation, which proposed that a homogeneous blend of two phases in presence of transesterification was form.
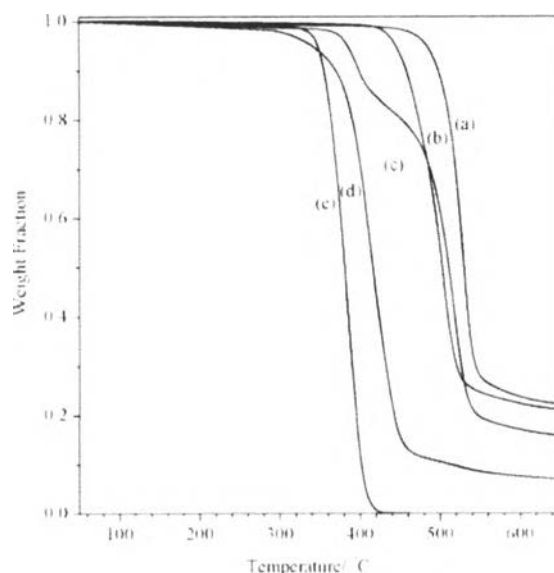
Figure 2.10 TGA of (a) PC bead, (b) extruded PC, (c) PC/20PMMA blend, (d) PC/20PMMA blend with 0.3% $SnCl_2.2H_2O$ and (e) pure PMMA.

Figure 2.11 presented the XRD patterns of melt extruded PC, PMMA and PC/PMMA blend with 0.3% $SnCl_2.2H_2O$ which all patterns showed the amorphous nature of pure phases and the blends because of the quenching effect. The two inset of Figure 2.11 revealed the variation of the position of the characteristic peak of PC with PMMA. As can be seen from the two insets in Figure 2.11, the PMMA content increased for fixed transesterification catalyst content at 0.3% (wt/wt), the peak of PC shifted toward lower 2θ angle. It can indicate that interchain spacing was increasing with increasing PMMA content. Moreover, for a fixed blend composition (PC/20PMMA) as well, the peak of PC shifted toward lower 2θ angle with increasing transesterification catalyst content. These supported graft copolymer formation, which was expected to increase the interchain spacing.
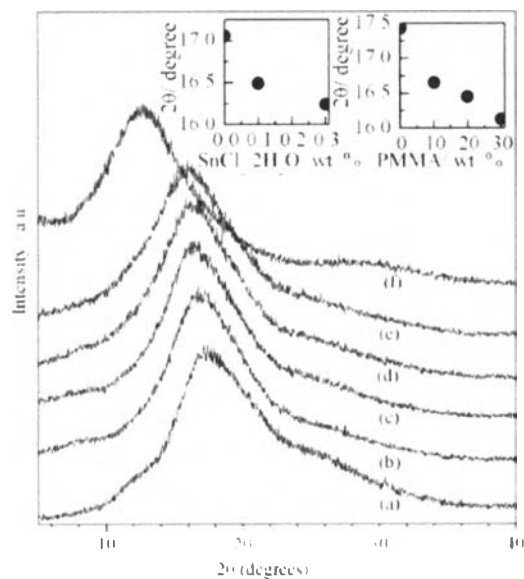
Figure 2.11 Powder XRD pattern of: **(a)** pure PC, **(b)** PC/10PMMA, **(c)** PC/10PMMA + 0.3% $SnCl_2.2H_2O$, **(d)** PC/20PMMA + 0.3% $SnCl_2.2H_2O$, **(e)** PC/30PMMA + 0.3% $SnCl_2.2H_2O$ and **(f)** pure PMMA prepared by melt extrusion method. Insets show the variation of the position of the characteristic PC peak as a function of transesterification catalyst content for PC/20PMMA blend composition and the PMMA content.

The optical transparency properties of pure PC, PC/10PMMA and PC/10PMMA with 0.3% $SnCl_2.2H_2O$ as shown in Figure 2.12 were measured by using UV/vis spectrophotometer. The optical transparency of PC was found to be about 85% in the 400-900 nm regions. In contrast, the optical transparency of PC/10PMMA blends without transesterification catalyst was found to be around 20% only for 900 nm wavelengths and it further decreased for the lower wavelengths. Consequently, it was noticed that by adding 0.3% $SnCl_2.2H_2O$ to the PC/PMMA blend, optical transparency enhanced significantly.
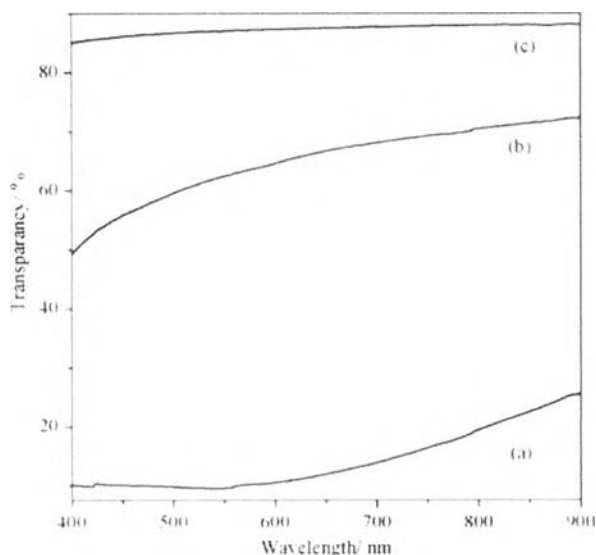
Figure 2.12 Optical transparency of: **(a)** PC/10PMMA, **(b)** PC/10PMMA + 0.3% $SnCl_2.2H_2O$ and **(c)** pure PC having film thickness of 0.6 mm.

The AFM images of PC/20PMMA blends without and with 0.3% $SnCl_2.2H_2O$ were shown in Figure 2.13. Granular morphology was seen in PC/20PMMA blends without $SnCl_2.2H_2O$, on the other hand homogeneous lamellar morphology was observed in PC/20PMMA blends with $SnCl_2.2H_2O$. It could be conclude that the prepared PC/PMMA blends in presence of transesterification catalyst $SnCl_2.2H_2O$ worked more efficiently than the organometallic transesterification catalysts known until date. Only 0.1% $SnCl_2.2H_2O$ was enough to set up an interaction between PC and PMMA phases, which led to homogeneous blend formation with single T_g. For the PC/PMMA blend that had PC-g-PMMA graft copolymer formation, which acted as a compatibilizer, these blends showed significantly higher transparency with respect to the uncompatibilized blends and homogeneous lamellar morphology.
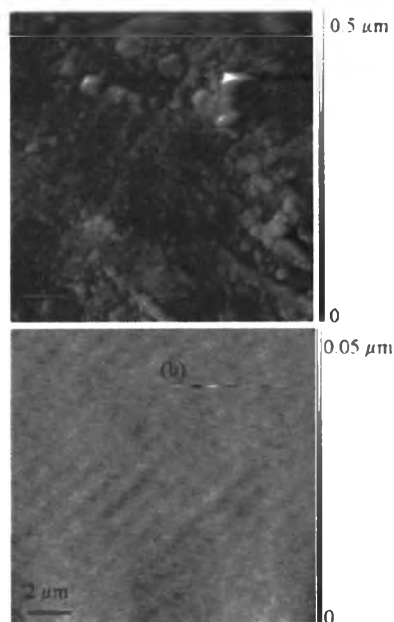
Figure 2.13 AFM image of (a) PC/20PMMA and (b) PC/20PMMA + 0.3% $SnCl_2.2H_2O$ blend.

2.6.2 Non-reactive compatibilization

In general, this process will improve the compatibility of the polymer in blending by adding the third component, which decreases interfacial tension and increases interfacial adhesion in the blend.

In 1992, Mekhilef *et al.* studied the effect of the addition of ionomer (EMAA) on the phase behavior of PC/PMMA blend. The ionomer was blend with PC/HDPE (80/20) blend by varying ionomer content at 1, 3 and 5%wt. The ionomer was an effective compatibilizer for PC/HDPE blend. It was because the interaction between PC and the ionomer was reactive and the structure of the ethylene side of ionomer similar to the polyethylene. Figure 2.14 presented the Young's Modulus based on the amount of ionomer when the ionomer content increased, the Young's Modulus tend to increase. Moreover the tensile strength increased by adding 1% of surlyn. More than 1%ionomer, however, the tensile strength seemed to decrease as shown in Figure 2.15. Hence, the addition of only 1% ionomer not only increased the

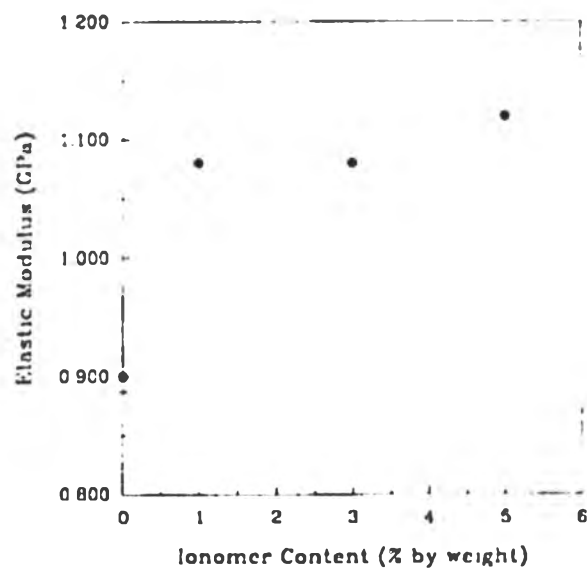Young's Modulus of the blend, but the tensile strength was also increased by almost 30%.

Figure 2.14 Effect of ionomer (EMAA) content on the Young's modulus of the blend.
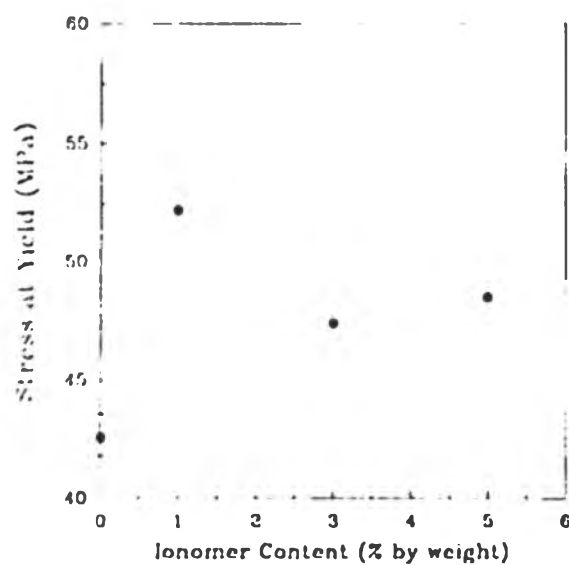

Figure 2.15 Effect of ionomer (EMAA) content on the tensile strength of the blend.

The SEM images of PC80/HDPE20 containing 0, 1, 3 and 5wt% ionomer were shown in Figure 2.16, respectively. From these results, they were found that the morphology was change after adding ionomer. In the case of more than 1% of ionomer, the morphology changed and became coarser with more elongated interface correspoonding to the result of tensile strength, which reduced when the amount of ionomer was more than 1%.
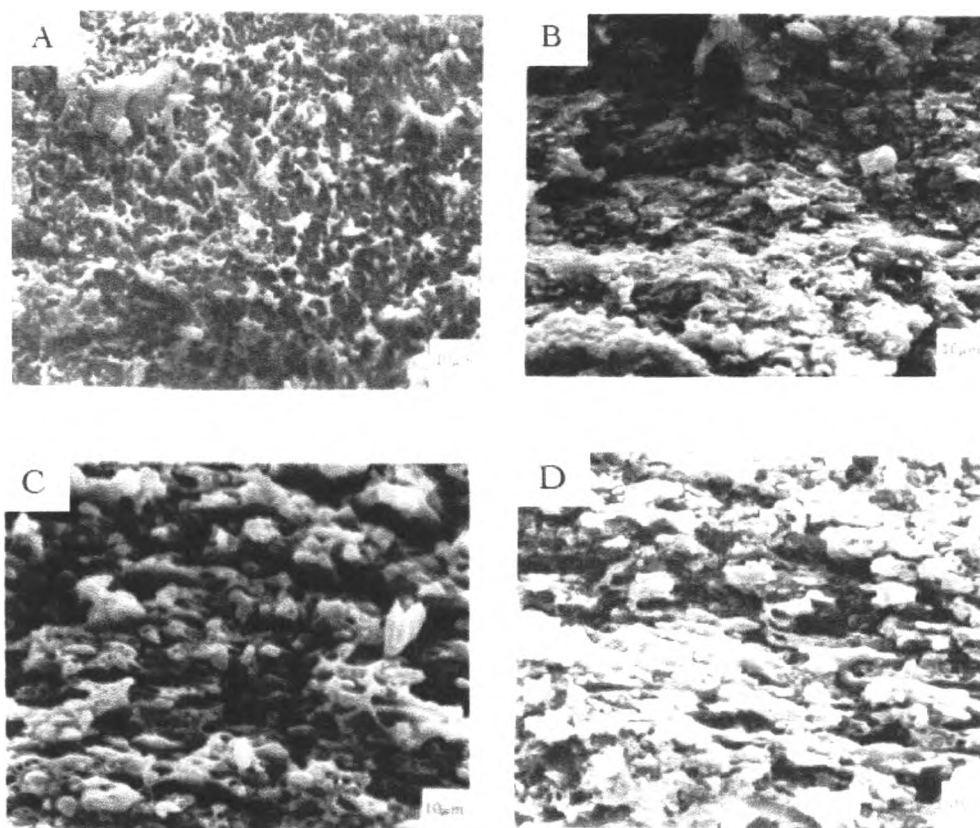

Figure 2.16 The SEM images of PC/HDPE 80/20 blend containing 0(A), 1(B), 3(C), 5(D) wt% ionomer (EMAA)

It could be conclude that blending of PC and HDPE with 1%ionomer resulted in the mechanical properties and the morphology was enhanced.

In 2010, Inpota *et al.* studied the effect of PC/PET alloys with various EMA contents on the mechanical properties and thermal properties. The PC/PET blends with different weight ratio were prepared by mixing in twin screw

extruder. EMA was used as a compatibilizer since it was a copolymer having acrylate part that could react with hydroxyl groups of PC and PET. From DSC results as given in Table 2.5, they were found that the two distinct T_g was observed at all alloys except PC20 which showed only one T_g corresponding to T_g of PET. Then, PC/PET/EMA alloys showed immiscible alloys.

Table 2.5 DSC results of PC/PET alloys with EMA

Formula	$T_{g,PET}$ (°C)	$T_{g,PC}$ (°C)	T_m (°C)	T_c (°C)	ΔH_m (J/g)	ΔH_c (J/g)	Crystallinity (%)
PC80	81.3	141.7	233.2	146.8	7.12	10.38	5.08
PC80 5EMA	83.2	144.6	252.6	149.2	1.30	14.59	0.93
PC80 10EMA	83.2	142.6	233.8	148.5	1.66	0.81	1.18
PC80 15EMA	82.3	143.4	233.4	144.5	1.93	2.96	1.38
PC50	81.6	Δ	238.6	148.7	22.55	10.07	16.10
PC50 5EMA	82.0	135.8	236.8	158.7	18.60	20.07	13.28
PC50 10EMA	82.6	136.1	239.3	154.6	15.26	12.85	10.89
PC50 15EMA	83.1	139.8	238.8	152.7	13.26	11.88	9.46
PC20	83.2	Δ	241.4	156.7	27.69	15.79	19.76
PC20 5EMA	83.5	Δ	237.6	149.7	25.01	4.04	17.85
PC20 10EMA	82.9	Δ	236.4	150.3	19.48	2.71	13.90
PC20 15EMA	82.7	Δ	234.7	150.9	19.99	1.28	14.27

ΔH of 100% crystalline PET is 140.1 J/g.

Δ $T_{g,PC}$ was duplicated by cold crystallization temperature (T_{cc}).

According to the impact testing, the toughness of PC/PET alloys with EMA were improved as can be seen in Figure 2.17. It was because the ethylene parts of EMA elastomer controlled the elastic properties and the effect of the interaction between hydroxyl groups at the chains end of PET and methacrylate groups of EMA. In addition, the impact strength of PC/PET alloys with EMA was evidently increased because the EMA had acrylate groups that could link between PC and PET, which the composition at PC80 with 5%EMA demonstrated the highest impact strength. In

the case of the higher EMA content, the trend of impact strength decreased due to the large amount of elastomeric EMA.
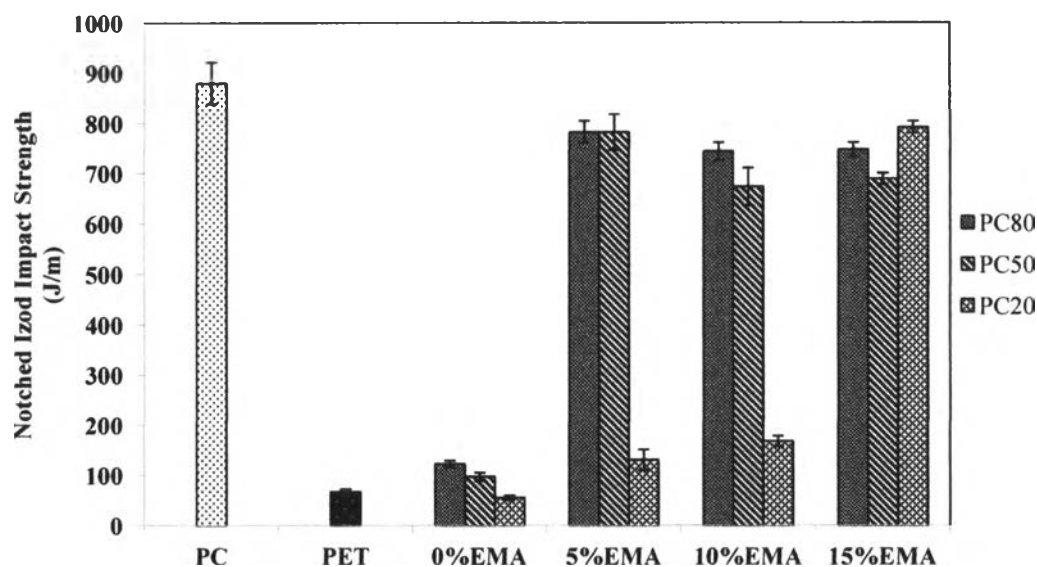

Figure 2.17 Notched izod impact strength of PC/PET alloys with EMA.

From these results, even though the addition of EMA did not improve the miscibility of PC/PET blends due to the appearance of two distinct T_g, it helped enhance the impact strengths significantly. Thus, it suggested that EMA could increase the interfacial adhesion between PC and PET led to the increasing in impact strength.

In 2013, Zhang *et al.* studied the effect of the various content of the reactive elastomer, ethylene/methyl acrylate/glycidyl methacrylate terpolymer (EMG), on the morphology and toughness of PLA. The SEM micrographs of cryofractured surfaces of PLA/EMG blends exhibited the phase separation at all blends. The EMG particles dispersed in PLA matrix which a large increase in the particle size was observed by increasing the EMG contents due to the coalescence of EMG phase as can be seen in Figure 2.18
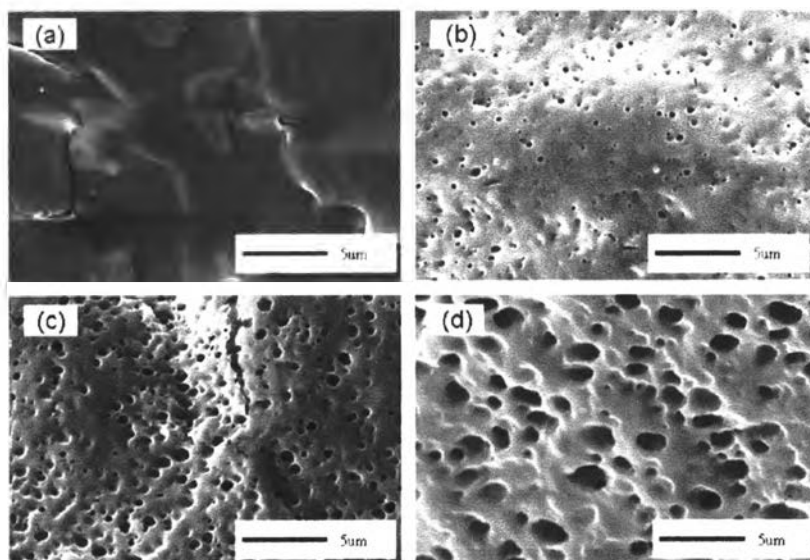
Figure 2.18 SEM images of etched surface of PLA/EMG blend with various samples: (a) neat PLA, (b) PLA10, (c) PLA20 and (d) PLA30.

Table 2.6 Mechanical properties of PLA and PLA/EMG blends

Samples	Modulus (MPa)	Tensile strength (MPa)	Elongation at break (%)	Impact strength (kJ m^{-1})
Neat PLA	1745 ± 39	60.0 ± 3.0	4.9 ± 0.3	3.0 ± 0.4
PLA10	1530 ± 35	44.3 ± 2.1	23.4 ± 3.6	3.9 ± 0.3
PLA20	1154 ± 42	33.8 ± 2.4	242.0 ± 26	59.8 ± 5.1
PLA30	945 ± 49	24.9 ± 1.3	126.0 ± 21	53.2 ± 8.4

For the mechanical properties, the stress-strain curves of neat PLA showed a feature of glassy and rigid materials as can see in Figure 2.19. It exhibited a yield point with following failure without necking at low elongation. However, the ductility of PLA was significantly improved by adding EMG and the fracture behavior of the blends showed the transition from brittle fracture to ductile. When the EMG contents increased, the yield stress of the blends decreased in contrast to their elongation at break increased significantly compared with those of neat PLA. In the case of modulus, it was likely to decrease because of the incorporation of the elastomeric EMG phases into the PLA matrix. In addition, EMG could improve the impact strength of the blends significantly which the increment of EMG contents in the blends resulted in an increase in toughness as can be seen in Table 2.6. According to Figure 2.20, the impact-fractured surface of neat PLA showed a brittle with smooth

surface. For the fracture surface of the blends, it showed the roughness surface with no clear separate particles of EMG when the amount of EMG increased. So it can be noted that there was a good adhesion between the PLA matrixes and the dispersed EMG phases.
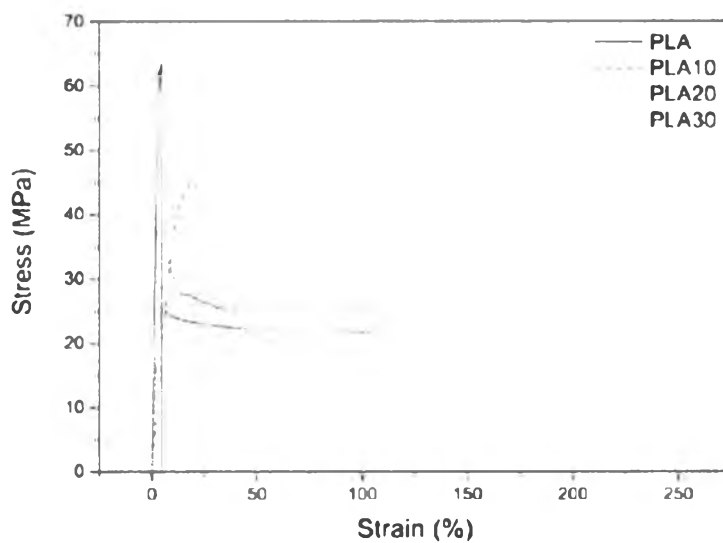

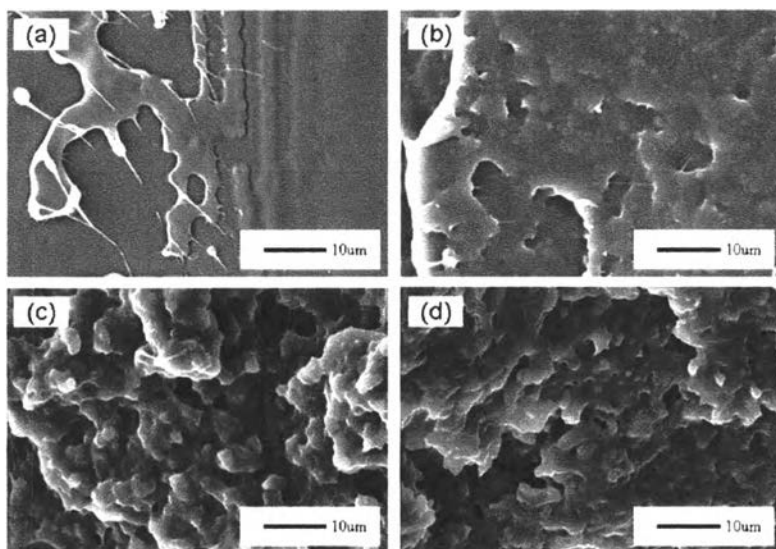**Figure 2.19** Stress-strain curves of neat PLA and PLA/EMG blend samples.

Figure 2.20 SEM images of impact-fractured surface of PLA/EMG blend with various samples: (a) neat PLA, (b) PLA10, (c) PLA20 and (d) PLA30.